J. Fluid Mech. (1977), *vol.* 79, *part* 1, *pp.* 191–208
Printed in Great Britain

Self-diffusion of particles in shear flow of a suspension

By EUGENE C. ECKSTEIN,† DOUGLAS G. BAILEY‡ AND ASCHER H. SHAPIRO

Department of Mechanical Engineering, Massachusetts Institute of Technology, Cambridge

(Received 31 March 1976 and in revised form 21 July 1976)

Self-diffusion coefficients were determined experimentally for lateral dispersion of spherical and disk-like particles in linear shear flow of a slurry at very low Reynolds number. Using a concentric-cylinder Couette apparatus, recurrent observations were made of the lateral position of a particular radioactively labelled particle. The self-diffusion coefficient D was calculated by means of random-walk theory, using the ergodic hypothesis. Owing to great experimental difficulties, the calculated values of D are not of high accuracy, but are correct to within a factor of two. In the range $0 < \phi < 0{\cdot}2$, $D/a^2\omega$ increases from zero linearly with ϕ up to $D/a^2\omega \cong 0{\cdot}02$ (where ϕ = volumetric concentration of particles, a = particle radius, ω = mean shear rate of suspending fluid). In the range $0{\cdot}2 < \phi < 0{\cdot}5$, the trend of $D/a^2\omega$ is not clear because of experimental scatter, but in this range $D/a^2\omega \cong 0{\cdot}025$ to within a factor of two. Within the experimental accuracy, spheres and disks have the same value of $D/a^2\omega$.

1. Introduction

Definition of the problem

A slurry is a relatively concentrated suspension of solid particles in a liquid. Suspensions may also consist of solid or liquid particles in a gas. As the particles are usually small relative to the size of the flow apparatus, certain average bulk properties of the mixture, such as density, effective viscosity and effective conductivity, are of obvious interest and importance (Goldsmith & Mason 1967; Brenner 1970; Batchelor 1974). Here we are particularly concerned with the fact that in a suspension flow the fluid-mechanical interactions among neighbouring particles produce irregular motions. Among these motions are lateral migrations from the instantaneous average trajectories, which produces an overall effect of dispersion.

The objective of the research reported here was an experimental determination of the self-diffusion coefficient characterizing the lateral migrational fluxes, under the especially simple conditions of an infinite linear shear flow.

† Present address: Biomedical Engineering Program, University of Miami, Coral Gables, Florida 33124.

‡ Present address: Foster-Miller Associates Inc., Waltham, Massachusetts 02154.

Practical significance

In industrial applications, suspensions provide an economical way of transporting large quantities of solid particulate materials. Well-known examples include coal and ore transport in mines and processing plants, pulp handling in paper manufacture, transport of powders in cement plants and the motion of particles in fluidized beds.

The most ubiquitous – indeed the most vital – slurry is blood, which contains within a suspending plasma a high volume fraction ($\sim 0{\cdot}4$) of particles (mainly red blood cells, but also platelets and white cells). Self-diffusion of the particles in blood is of great importance in at least three respects.

(i) In extracorporeal devices, red cells are haemolysed when they come into contact with artificial surfaces.

(ii) The formation of clots, or thrombi, is in part determined by the diffusional fluxes of platelets to the walls.

(iii) Since oxygen is largely transported by attachment to the haemoglobin of red cells and subsequent movement of the red cells, the self-diffusion of red cells produces augmented diffusion as, for instance, in blood oxygenators. Self-diffusion moves oxygen-saturated red cells to unsaturated regions; this 'bucket brigade' produces an increased rate of mass transfer.

The rheological and diffusive behaviour of blood presents the additional complications of deformability of the particles and of protein linkages at low shear rates, both producing non-Newtonian behaviour (Merrill *et al.* 1963; Whitmore 1963; Fung 1969; Copley 1966; Charm 1974).

How diffusive-type lateral migrations arise

Particle motions perpendicular to the local direction of flow may arise from three sources (Cox & Mason 1971): (i) *mutually induced velocity fields* during a shear flow (Goldsmith & Mason 1967; Karnis, Goldsmith & Mason 1966*a*), (ii) *lift forces* (Segre & Silberberg 1962; Ho & Leal 1974; Wohl & Rubinow 1974; Karnis, Goldsmith & Mason 1966*b*) and (iii) *body forces*, e.g. gravity or centrifugal forces.

Motions due to lift and body forces can be present even in very dilute suspensions. They are not stochastic, and are best quantified in terms of a drift speed rather than by a self-diffusion coefficient.

Only those particle migrations associated with mutually induced velocity fields are the object of study here. These produce self-diffusion even in an infinite linear shear flow of uniform concentration, and in the absence of buoyancy forces, nonlinear shear, fluid inertia and wall proximity. The essential requirement is that the particle concentration be sufficiently high to result in a significant number of multi-particle interactions.

A simple, linear shear flow of a suspension continually produces two types of interaction, both of which contribute to lateral migrations.

(i) Each particle rotates with an angular velocity approximately half the mean shear rate of the fluid (Jeffery 1922). Because of viscous entrainment a

circulatory fluid motion is established around the particle, thereby creating a velocity field that exerts drag forces on neighbouring particles. (ii) Each particle overtakes and passes particles on neighbouring but slower-moving mean streamlines, and is passed by particles on faster-moving mean streamlines. In such passing encounters or 'collisions' (usually without contact), each particle moves in the velocity field of its neighbours. With only two particles present and far from bounding walls, a passing encounter at zero Reynolds number is symmetrical: neither particle experiences a *net* lateral displacement, even though there may be large temporary displacements as the particles move to avoid each other during the passing event. With many particles present, the beginnings and ends of the multiple passing interactions overlap and are indistinct, but the important fact is that net lateral displacements do occur (Goldsmith & Mason 1967).

Representation of the phenomenon as self-diffusion

We make the plausible supposition that the arrangement of particles which are near neighbours is a continuously changing random event. Then, since both contributions to the lateral migrations, i.e. the rotational and the translational contributions, are created by many successive inputs, with each input arising from a different random arrangement of neighbours, the self-diffusion of the particles should exhibit the type of statistical behaviour associated with random-walk processes. Accordingly, the dispersive behaviour may be characterized quantitatively by Fick's law of diffusion in terms of a coefficient of self-diffusion.

Considered in this light, the self-diffusion of particles in shear flow of a slurry resembles both the molecular collisions that give rise to ordinary diffusion in a gas and the fluid-mechanical events that produce dispersion and mixing in a turbulent flow. Both analogies, however, while somewhat helpful as an aid to thought, are imprecise. The physical phenomena involved are quite different for the three cases, although Buyevich (1972) attempted to calculate shear-induced dispersion in slurries through an analogy with turbulent flow.

Dimensional analysis

A given flow geometry, e.g. a pipe or slit flow, or a cylindrical Couette flow, may be characterized by a typical width w. Let the local shear rate be $\omega \equiv \partial u/\partial y$ at the distance y from the wall. We consider cases where the mean flow is approximately rectilinear on the scale of the inter-particle spacing, so that it may be characterized by an average velocity profile $u(y)$. Then, with respect to particle interactions, the local mean flow at y is determined by the successive derivatives $\partial u/\partial y$, $\partial^2 u/\partial y^2, \ldots$. For nearly linear shear flows, one presumably need not go beyond $\partial^2 u/\partial y^2$. Additional variables entering the diffusive behaviour are the particle radius a, the average volumetric concentration ϕ, the fluid viscosity μ, the mass density of the fluid ρ_f and the net body force, which is proportional to $g(\rho_s - \rho_f)\, a^3$, where g is the body force per unit mass (gravitational, centrifugal, etc.) and ρ_s is the mass density of the particles.

The average coefficient of self-diffusion D is governed by the foregoing quantities through the implicit physical relationship

$$D = D[\phi, a, w, y, \omega, \partial^2 u/\partial y^2, \mu, \rho_f, g(\rho_s - \rho_f)\, a^3]. \tag{1}$$

Dimensional arguments reduce this to

$$\frac{D}{a^2\omega} = \mathscr{D}\left[\phi, \frac{a}{w}, \frac{a}{y}, \frac{\rho_f a^2 \omega}{\mu}, \frac{a\,\partial^2 u/\partial y^2}{\omega}, \frac{g(\rho_s - \rho_f)\, a}{\mu\omega}\right]. \tag{2}$$

The geometric parameters a/w and a/y are obviously related to wall interference effects. The term $\rho_f a^2\omega/\mu$ is the appropriate Reynolds number of the flow relative to a particle when the slip velocity is very small; it also governs the rate of decay of a non-equilibrium slip velocity. The group $a\,\partial^2 u/\partial y^2/\omega$ is a measure of the fractional change in shear rate over a distance of one particle radius; if this term is non-zero, an equilibrium slip velocity as well as a transverse lifting force is produced (Ho & Leal 1974). The last dimensionless parameter, $g(\rho_s - \rho_f)\, a/\mu\omega$, is a measure of the ratio of the settling speed (in the direction of g) produced by the unbalanced body force to the speed ωa characterizing the local shear flow relative to a particle.

Objective and scope

Even in a pipe flow, a multitude of complex and interacting phenomena enter. The nonlinear velocity profile produces tranverse lift forces. This, together with interference effects near the walls, results in a non-uniform distribution of particle concentration. The consequent gradient of concentration influences the diffusive effects due to particle interactions. Experiments in pipes and channels, because of the presence of such multiple and interacting phenomena, are difficult to interpret, particularly with respect to determination of the coefficient of self-diffusion. Experiments with blood have additional complications owing to the deformability of the red cells, leading for instance to an apparent non-Newtonian viscosity.

It was our objective to perform experiments in which self-diffusion is the dominant physical phenomenon, essentially free of other effects. As described later in more detail, the experiments were performed in a cylindrical Couette apparatus having a small ratio of gap width to mean radius, using small, virtually neutrally buoyant particles suspended in a very viscous oil. Measurements were made only in the central region of the gap, where the velocity profile was nearly linear and the concentration nearly uniform. Under the experimental conditions, all the independent dimensionless parameters in (2) except ϕ were quite small. If each were truly zero, the problem would be that of an infinite, inertia-free, two-dimensional, neutrally buoyant, linear shear flow, with the particle migrations wholly governed by self-diffusion of the type described earlier. In that case (2) would reduce to

$$D/a^2\omega = \mathscr{D}[\phi], \tag{3}$$

a situation to which the experiments approximated.

The experimental investigations were carried out by Eckstein (1975), using rigid spheres, and Bailey (1975), using rigid discoids, whose theses may be consulted for fuller details than can be presented here.

2. Related investigations

Quantitative information concerning the self-diffusion coefficient in a linear shear flow is virtually non-existent. Experimental studies have not been aimed towards this goal, and not even the beginnings of a workable theory are available to model the complex phenomena involved. However, various related studies reported in the literature bear more or less upon the present investigation.

Individual particles in a shear flow

Brenner (1963) and Happel & Brenner (1973) describe well-established results for single neutrally buoyant particles. In an unbounded linear shear flow the particle's speed is that of the streamline at its centre, and its angular velocity is half the fluid shear rate (see also Jeffery 1922). Proximity to a solid boundary reduces both the convective speed and the angular velocity. In an inertia-free flow, a rigid particle experiences no lift force even near a solid boundary, in accord with the principle of kinematic reversibility (Bretherton 1962; Cox & Mason 1971). However, with significant inertial effects, i.e. at non-zero particle Reynolds number, the interference effect of the wall does yield a lift force. Deformable particles or immiscible liquid droplets experience lift forces whatever the Reynolds number. Lift forces on rigid particles are smaller than those on similar deformable particles or droplets.

Concentrated suspensions in shear flow

Experiments in cylindrical Couette flows and in Poiseuille flows are reviewed by Goldsmith & Mason (1967). While a two-particle interaction produces no net lateral migration in a linear shear flow, observation shows that net lateral migrations do occur when three or more particles are present (Karnis *et al.* 1966*a*). The dispersive-type motions increase greatly as the volumetric concentration of particles increases from dilute values. Kinematic reversibility, which bears a close relationship to dispersive particle migrations, fails above a Reynolds number $\rho_f a^2\omega/\mu$ of 10^{-5}. This is much smaller than one would expect if, say, the velocity field or the drag, both instantaneous quantities, were the quantities of interest. However, the return of a particle to its initial position when the flow is reversed relates to an integral measure which can be substantially affected by small but cumulative deviations.

Couette flows. Observations by Karnis *et al.* (1966*a*) showed that the concentration within a Couette channel in an inertia-free flow is virtually uniform, except for a 'Vand zone' of low concentration near each wall (Vand 1948). The velocity profile, however, is of complex shape: it consists of an essentially linear central region bounded by regions of much higher shear rate in the Vand zones.

This shape results from the combination of a nearly constant shear stress across the entire gap and an effective viscosity that is non-uniform owing to the deficiency of concentration in the Vand zone.

Poiseuille flows. When a low-concentration suspension of neutrally buoyant particles issues uniformly from a reservoir into a tube, the particles migrate radially and ultimately assume a stable position at a radius of approximately 55 % of the tube radius (Segré & Silberberg 1962). The suspension is relatively depleted of particles near the wall and in the centre (Cox & Mason 1971). The 'Segré–Silberberg effect' involves a balance between two competing transverse lift forces: that arising from curvature of the velocity profile and that owing to inertial effects in the presence of wall interference (Ho & Leal 1974). Flows of neutrally buoyant suspensions at high concentrations have been the subject of visual studies by Karnis *et al.* (1966*b*) and by Sacks & Tickner (1967). Above a tube Reynolds number of 10, a slurry of high concentration exhibits plug-flow behaviour in the centre bounded by a high shear flow in a wall region depleted of particles. The lateral migrational motions in the plug portion of the flow are much smaller than in the wall region of high shear.

Augmented diffusion in blood flow

In considering the results of experiments on thrombus formation in a stagnation-point flow, Petschek & Weiss (1970) postulated a shear-driven diffusion of the platelets, presumably by action of the red cells. Experimental attempts to relate wall-induced haemolysis to the self-induced diffusion of red blood cells in tube flows were made by Bernstein, Blackshear & Keller (1967) and by Steinbach (1974), with somewhat puzzling results, perhaps due to the inherent complexities of tube flows of suspensions, discussed earlier, as well as to the effects of the great flexibility of red cells. In experiments using the method of Taylor (1953) to measure the diffusion of platelets, Turitto, Benis & Leonard (1972) found the diffusion coefficient in a flowing system to be much larger than the molecular diffusion coefficient of a static suspension. Grabowski, Friedman & Leonard (1972) investigated the effect of the shear rate on platelet-thrombus formation in the presence of red blood cells.

The diffusive migration of red blood cells in a shear flow and the associated augmentation of diffusive transport of dissolved species in the plasma offer a potential method for significantly reducing the size of blood oxygenators (Colton 1976; Collingham 1968; Diller 1974; Keller 1971; Hill *et al.* 1974).

3. Experimental apparatus

General considerations

Although self-diffusion in a slurry is known to occur, the experimental determination of the coefficient of self-diffusion imposes formidable difficulties. In a developed pipe flow, for instance, there are the complications of a non-uniform concentration (due to the Vand zone and the Segré–Silberberg effect) and a nonlinear velocity profile. Even in a simpler flow, how can one make observations,

in a cloud of supposedly identical particles, from which any sort of self-diffusion coefficient may be extracted?

Our desire was to approximate as nearly as possible the most elementary circumstances in which self-diffusion is the dominant feature. This is an unbounded linear shear flow of a slurry of rigid particles neutrally suspended in a Newtonian fluid at uniform concentration, with inertial effects negligible. The chief elements in the experimental plan were a cylindrical Couette device having a small gap/radius ratio, a suspension of small plastic particles in a very viscous oil matched to the density of the particles, and a system for detecting the lateral position within the Couette gap of one tracer particle that had been labelled radioactively but was otherwise similar to the other particles.

The selection of dimensions, rotational speeds, viscosities, densities, etc., was governed by the restrictions implied by the simple relation (3), as well as by considerations of practicality and convenience. These restrictions and considerations produced in the eventual design the following ranges or values of the independent dimensionless parameters in (2):

$$\begin{aligned} \phi &= 0{\cdot}054 \text{ to } 0{\cdot}50, \\ \rho_f \omega a^2/\mu &= 4 \times 10^{-4} \text{ to } 10^{-2}, \\ |g(\rho_s - \rho_f)\, a/\mu\omega| &= 0{\cdot}004 \text{ to } 0{\cdot}06, \\ a/w &= 0{\cdot}02 \text{ and } 0{\cdot}06, \\ a/y &= 0{\cdot}05 \text{ and } 0{\cdot}15 \text{ (approx.)}. \end{aligned}$$

The value of $a\,\partial^2 u/\partial y^2/\omega$ is difficult to establish. However, from the results of Karnis *et al.* (1966*a*) it was possible to estimate the size of the wall regions, and thus of the region where the velocity profile is virtually linear. Accordingly, only migrations of the marked particle originating in the central fifth of the channel width were used for calculating D, and it is believed that the associated values of $a\,\partial^2 u/\partial y^2/\omega$ were sufficiently small to be considered essentially zero.

The ratios listed above are a compromise between the ideal of (3) and what is practically realizable. Although the parameters in (2) (except for ϕ) may have not been rendered wholly inconsequential, they are deemed to have had a relatively weak influence on the measured value of D.

The concentric-cylinder Couette apparatus

The Couette apparatus was of conventional design, but constructed with a high degree of mechanical accuracy. The significant dimensions were inner diameter = 10·98 in., outer diameter = 13·05 in., gap width = 1·053 in. and maximum possible fluid height = 9·8 in. The bottom rotated with the outer cylinder, and the upper horizontal surface of the slurry was in contact with air. Except for the experiment with $\omega = 0{\cdot}4\,\mathrm{s}^{-1}$, the inner cylinder was stationary. For $\omega = 0{\cdot}4\,\mathrm{s}^{-1}$, both cylinders rotated, the speed of the outer cylinder being the same as in the experiments having $\omega = 1{\cdot}0\,\mathrm{s}^{-1}$.

In rotating Couette devices, the existence of a boundary layer on the floor leads inevitably to a toroidal secondary circulation in a diametral plane. Such

a secondary flow, unless exceptionally small, would be disastrous for the present experiment, as it would cause first-order particle displacements that could easily mask the second-order shear-induced migrations. In order to render the secondary flow negligible, a layer of 'Fluorinert' (3M Co.) about 4·5 in. deep was placed at the bottom of the Couette chamber. This totally fluorinated hydrocarbon is 65 % more dense than the slurry used (thereby minimizing instabilities and wave formation at the interface) and, most important, is at least 1000 times less viscous. Thus, because the shear stress is continuous at the interface, the secondary flow was in effect confined to the Fluorinert layer. The air–slurry interface acted in a similar manner to prevent secondary flow within the slurry.

Furthermore, in order to avoid thermal convection currents, the entire apparatus was operated in a thermostatically controlled room.

With these precautionary steps, no secondary or thermal flow effects could be detected in 2 h observations of a simple, small, neutrally buoyant particle moving in the viscous suspending fluid.

The slurries

In the experiments with spheres, the water-soluble artificial oil used, Ucon 50-HB-5100 (Union Carbide), was diluted with water until the fluid and particle densities matched to within less than 0·002 g/cm^3. At this condition, the viscosity of the solution was 2100 cP at 70 °F. In the experiments with disks the match was not quite as good.

Two sizes and two shapes of polystyrene particles were used. By means of a complex and difficult procedure, one of each type of particle was labelled with a sufficient amount of ^{58}Co so that it could be detected through the emission of 810 KeV gamma rays.

'*Large*' *spherical particles.* These were commercially manufactured by centreless grinding to diameters of $0{\cdot}125 \pm 0{\cdot}002$ in.

'*Small*' *spherical particles.* These were commercially produced by polymerization of drops in suspension. The particles used in the experiments were selected by sieving. Approximately 95 % of the particles had diameters between 0·038 and 0·045 in.

Disk-like particles. These were stampings from polystyrene sheet, with dimensions $2a = 0{\cdot}121 \pm 0{\cdot}001$ in. (approximately the diameter of the 'large' spheres) and $h = 0{\cdot}021 \pm 0{\cdot}003$ in. (a = radius, h = thickness), and with a density $\rho_s = 1{\cdot}057$ g/cm^3. Since the ratio $h/2a \cong 0{\cdot}17$, the disks were 'thin'.

Scheme for determining D

Recurrent observation of the position of a single marked particle as time proceeds permits a coefficient of self-diffusion to be calculated if one adopts the ergodic hypothesis. Because of the stochastic nature of the lateral migrations, the statistical behaviour over a sufficiently long time of one particle in a cloud of particles represents also the statistical behaviour of the entire cloud of particles over a short time. This is so because the marked particle at various later times occupies all the current positions of the particles making up the cloud.

It would have been advantageous to observe the lateral position of the radioactive particle within the Couette gap at uniform time intervals (neither too long nor too short, as explained later). To do this with adequate positional accuracy was not feasible without great complication of the apparatus. In the method adopted, the particle was observed only as it passed through a 'viewing window' occupying a small circumferential arc of the Couette annulus. By thus reducing the area of observation, the accuracy of determining lateral position was enhanced, but with the disadvantage that the time intervals between successive observations of the radioactive particle were not uniform and thus had to be measured.

Detection system

Each time the marked particle passed through the arc of the viewing window, a scintillation detector was activated, and data giving the lateral position of the particle within the gap and the time elapsed since the previous observation were recorded on tape.

The apparatus is shown schematically in figures 1 (*a*)–(*c*). For clarity, almost all the lead shielding has been omitted from the figures. Only the shielding making up the sides of the collimating slits in the rotating lead wheel F is retained in the figures. Additional lead shielding, not shown, protected the scintillation detector A from radiation not passing through the viewing slits.

Figure 1 (*c*) which is a sectional top view of figure 1 (*a*), shows the lower half of the rotating lead wheel, which contained the successive collimating slits through which the labelled particle could be viewed. The viewing slits were sufficiently spaced that only one slit could be over the Couette gap. As the lead wheel rotated, a small circumferential arc of the Couette annulus was repeatedly scanned by the slits, one at a time.

The scintillation detector A was placed directly over the viewing arc of the Couette annulus. Gamma rays emitted by the radioactive particle had a relatively decay-free path to the detector only when the lateral position of a viewing slit corresponded to the particle position. An electrical signal was generated in response to the high rate of gamma-ray counts registered by the radiation electronics whenever a slit was positioned directly over the radioactive particle. Measurement of the slit location thus determined the location of the radioactive particle.

As each collimating slit approached the Couette annulus, a light beam from the He–Ne laser B, after 90° reflexion by the mirror H, passed through the collimating slit to the photodiode D. Since the laser beam was fixed relative to the apparatus, the electrical signal from the photodiode established a reference location for the subsequent measurement of the position of the marked particle.

The electrical signal from the photodiode zeroed an electronic stop-watch, and the radiation-induced signal from the scintillation counter caused the stop-watch to record the time when the marked particle was observed. From the elapsed time (the lateral distance from the laser beam to the particle divided by the speed of the collimating slit) and knowledge of the location of the walls of the Couette gap relative to the laser beam (found by a preliminary calibration),

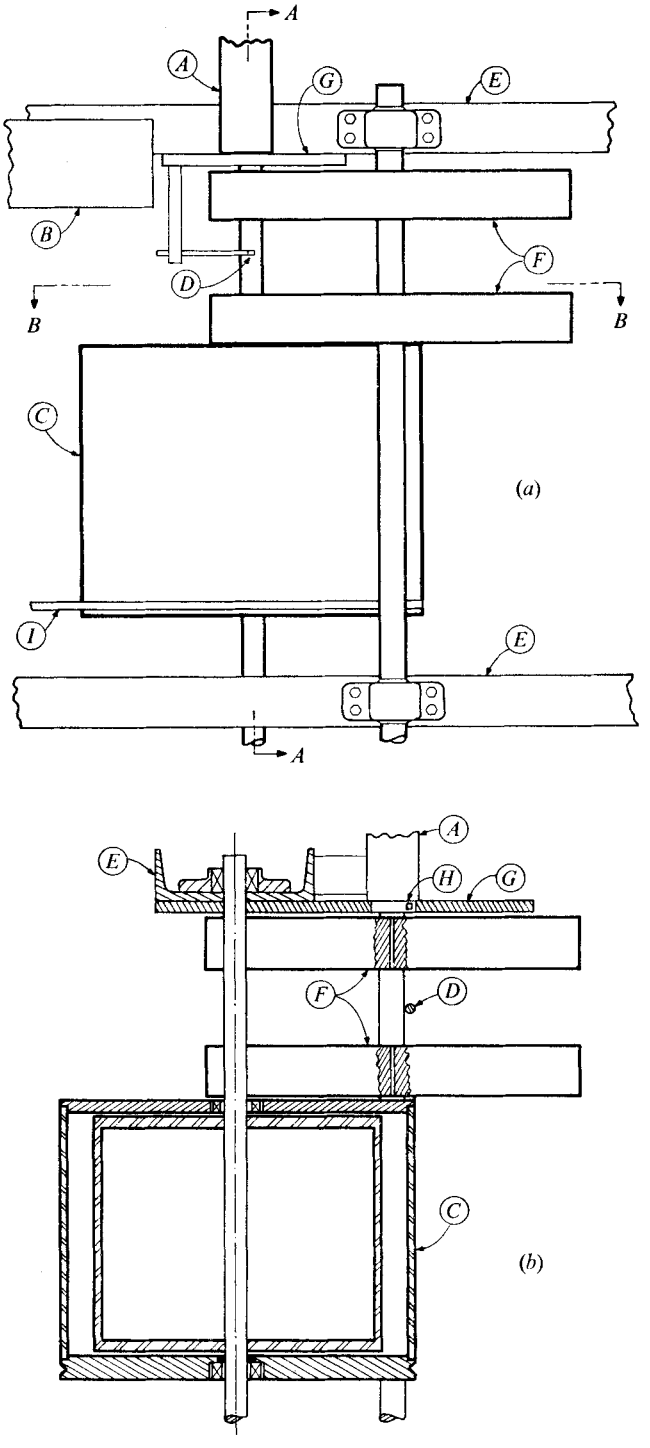

FIGURE 1. For legend see facing page.

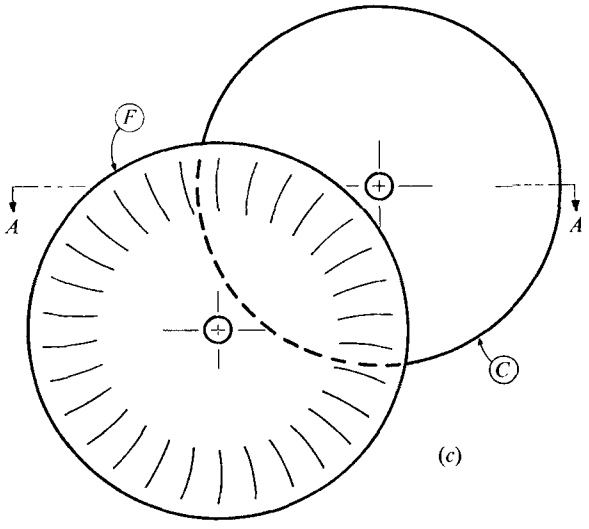

FIGURE 1. The Couette device and the detection apparatus. *A*, scintillation counter; *B*, He–Ne laser; *C*, Couette device; *D*, photodiode; *E*, steel frame; *F*, lead wheels with collimating slits; *G*, shelf for lead shielding (the latter not shown); *H*, 90°-turn mirror; *I*, belt drive for outer Couette cylinder. (*a*) Front view. (*b*) Side sectional view (section *AA* of *a*). (*c*) Top view (section *BB* of *a*), showing only the outline of the Couette device and the lowermost lead wheel with collimating slits.

the position of the labelled particle relative to the walls of the Couette gap could be determined.

In addition to the scintillation counter, the radiation detection equipment included a spectrometer which filtered out pulses produced by gamma rays outside the 810 keV band.

Co-ordinating electronics

An electronic interface, constructed principally from transistor–transistor–logic integrated circuits, processed the outputs of the spectrometer and photodiode, co-ordinated two stop-watch timers and prepared a coded output for a teletype. The interface acted as a small dedicated computer controlling the moment-to-moment collection of data.

The counts filtered through the spectrometer formed the input to a rate meter. The latter produced a pulse whenever the number of counts received in a 5 ms interval exceeded a preset threshold level. This pulse stopped two electronic stop-watches and also initiated automatic recording of the times on the teletype.

The 'position' stop-watch measured the time for the collimating slit to move horizontally from the reference laser beam to the location of the marked particle. It was reset to zero by the photodiode each time a new collimating slit reached the laser beam and began to scan across the Couette gap.

The 'interval' stop-watch measured the time interval between successive observations of the marked particle. It was reset to zero, and immediately restarted, when the counter sent a signal to memory that the marked particle had been detected.

Control and multiplexing circuitry integrated the functions of the electronic components with the teletype to provide automatic recording of observations. When the rate meter signalled a 'hit' as a collimating slit passed over the marked particle, several actions were simultaneously initiated: (i) the times of the two stop-watches were recorded in their respective memory sections; (ii) the interval stop-watch was zeroed and restarted (the position stop-watch was rezeroed by the photodiode); (iii) a code-conversion section translated the internal electronic signals into a form which could be recorded on paper tape through the teletype; (iv) an interlock prevented numbers recorded in the stop-watch memories from being lost while the teletype was producing the paper-tape record; and (v) a dead-time latch was set, preventing further observations until some minimum preset time had elapsed. The dead-time interval was made sufficiently great so that the current observation could be recorded by the teletype and also so that observations with very small lateral changes in particle position were avoided. The latter was important as a means of reducing certain sources of error which, as discussed later, would systematically produce erroneously large diffusion coefficients.

4. Treatment of data

Calculation of self-diffusion coefficient

Using the techniques and apparatus described above, data for each run were accumulated in the form of a table of lateral changes in position Δy_i and corresponding time intervals Δt_i. These data were treated as a series of random walks, at least with regard to lateral migrations. For random walks in one dimension, with unequal time intervals Δt_i, the self-diffusion coefficient is given by (e.g. Chandrasekhar 1943)

$$D = \frac{1}{2N} \sum_{1}^{N} \frac{(\Delta y_i)^2}{\Delta t_i}, \tag{4}$$

where N is the number of observations.

The observations used to form Δy_i must be uncorrelated. This requires that many collisions occur during the time interval Δt_i, a condition that was met automatically since in all experiments (except with $\omega = 0{\cdot}4\,\mathrm{s}^{-1}$) the radioactive particle had to move around the Couette annulus to return to the viewing window for another observation. The number of collisions can be estimated by considering the change in registration of the elements of a cubic crystalline array being sheared. The number of collisions is simply the number of elements passed, i.e. $\omega \Delta t_i$. In these experiments the number of collisions between observations is of the order of 100 or more, using the time interval described subsequently.

Straightforward as the experimental procedure may be in concept, it was fraught with practical difficulties, and contained pitfalls that could easily lead to spurious results. Only by careful consideration of the various sources of error, by appropriate procedures in both the taking and the treatment of data to cope with these and by a variety of calibrational and theoretical estimates of error

magnitude was it possible to arrive at values of D which do indeed represent self diffusion and which are reasonably correct in magnitude.

The major considerations of error are outlined briefly below (for full details see Eckstein 1975).

Systematic errors

These are principally in the determination of the shear rate ω and the concentration ϕ in the central region of the channel where the migrational observations were made. Errors in ω and ϕ are greater for the larger particles, since the latter produce wider wall zones where the concentration is lower and the shear rate higher than the respective average values.

Apparent shear rate. The values of ω used in reducing the data were based on a linear variation of fluid speed between the inner and outer walls. This neglects the rather small curvature in the velocity profile that would occur even with a homogeneous Newtonian fluid because the gap/radius ratio is not zero. More important, it neglects the fact that the shear rate in the centre is less than the average because of the regions of high shear near the walls. From the data of Karnis *et al.* (1966*a*), it is estimated that the associated error in $D/a^2\omega$ is not more than 20 % even for the tests with the larger particles.

Apparent volume concentration. The values of ϕ reported are the average for the entire slurry. In the central region of the channel where the diffusion measurements were made, the actual concentration is higher than the average. Using the assumption of a Vand-zone depleted layer one particle radius in width, the error in ϕ is estimated to be about 15 % for the larger particles and only a few per cent for the smaller particles.

A particular error with the small spheres. Although the radii of the small spherical particles ranged from 0·019 to 0·023 in. difficulties in fabrication caused the radioactively labelled sphere to be somewhat larger, of radius 0·026 in. The results were calculated using $a = 0{\cdot}023$ in. For this and other reasons discussed later, the results with the small spheres are not as reliable as those with the large spheres.

Random errors

These may be divided into two classes. The 'sighting' error is the customary difference between the actual position of the labelled particle and the position reported by the detector, and incorporates the usual errors of observation.

The second source of random error, the 'passing' error, is somewhat unusual. As the labelled particle successively passes (or is passed by) other particles, it executes an erratic, meandering motion. A portion of the lateral displacement is temporary (as exemplified by the isolated two-particle collision) and is lost at the conclusion of the encounter. Incorporation of this temporary displacement into the position observation would produce a spuriously high value of Δy_i with regard to self-diffusion. The values of Δy_i to be used in (4) should be based on an average trajectory free of temporary lateral displacements due to passing encounters. Since there is no way of separating out the temporary passing displacements, it is important to recognize that, as the time interval Δt_i increases,

the scale of the 'true' diffusive Δy_i increases in proportion to $(\Delta t_i)^{\frac{1}{2}}$, whereas the contribution of the 'passing' error to Δy_i remains constant.

Let the observed position y_{obs} of the particle be expressed as

$$y_{\text{obs}} = y_{\text{true}} + y_{\text{pass}} + y_{\text{sight}}, \tag{5}$$

where the last two terms represent the two sources of error discussed above. A corresponding expression holds for the respective Δy's. Assuming that each of the Δy's is random (the mean values are zero) and that they are independent of each other, substitution of (5) into (4) leads to

$$D_{\text{obs}} = D_{\text{true}} + \frac{1}{2N}\Sigma\frac{(\Delta y_i)^2_{\text{pass}}}{\Delta t_i} + \frac{1}{2N}\Sigma\frac{(\Delta y_i)^2_{\text{sight}}}{\Delta t_i}, \tag{6}$$

where D_{true} is the correct value based on the values of $(\Delta y_i)_{\text{true}}$.

Both contributions to the error in Δy_i, regardless of their signs, increase the value of D_{obs} over the correct value D_{true}.

Sighting errors. These are determined by (i) mechanical errors in alignment of the various components, (ii) the width and geometry of the viewing slits and the vertical position of the labelled particle, which determine the shape of the curve of count rate *vs.* time as the radioactive particle comes into view, (iii) the threshold count rate set for an observational 'hit', as this is related to the aforementioned curve, (iv) the size of the finite time slices within which the counts are successively accumulated by the rate meter and (v) various small inaccuracies in dimensions, speeds, stop-watch times, etc.

Observations were made of all particles attached at various points on the two walls of the Couette device. This provided an absolute reference base for the position of the laser beam relative to the walls. Additionally, it gave information on the statistics of the sighting error. The observed positions were centrally distributed around the mean, which was taken as the true position of the wall. For the large sphere and the disk, the breadth of the position distribution function was such that the observed position was accurate to within one particle radius in 95 % of the sightings. For the small sphere, several reasons combined to make the accuracy less: to within one or two particle diameters in 80 % of the sightings.

Passing errors. These are most difficult to assess. Presumably the error $(\Delta y)_{\text{pass}}$ lies between zero and approximately $2a$. As noted, the error in D diminishes as the time intervals Δt_i grow larger. Although very rough estimates of the passing error in D were made to ascertain that it was not disastrously large, the principal strategy used for coping with this vagary was to work with sufficiently large values of Δt_i.

Error as a function of time interval

Although (6) reveals the dismal fact that the passing and sighting errors, even though random, produce errors in D in only one direction (they would produce a spurious value of D even if there were no true diffusion!), they may be rendered relatively small by making Δt_i large enough, since both $(\Delta y_i)_{\text{pass}}$ and $(\Delta y_i)_{\text{sight}}$ are fixed in scale and independent of Δt_i.

The computer program which processed the data was capable of algebraically summing the values of $(\Delta y_i)_{\text{obs}}$ and Δt_i for a series of jumps, thereby yielding experimental data for jumps with successively larger Δt_i's. Thus it was possible to calculate D_{obs} for any allowed minimum interval $\Delta t_i = \Delta t_i^*$ between observations of the marked particle.

For small values of Δt_i^*, the computed value of D_{obs} is quite large, owing to the relatively weighty influence of the passing and sighting errors, as shown by (6). As Δt_i^* increases, these errors become less important, and D_{obs} decreases. In an infinite shear flow, D_{obs} would approach D_{true} as $\Delta t_i^* \to \infty$. But, because of the presence of walls in the apparatus, Δy_i is bounded, so that D_{obs} would in fact approach zero as $\Delta t_i^* \to \infty$. Long before this occurred, however, some of the particle positions would be within the wall layers.

Clearly, then, in order to provide a good approximation to D_{true}, the value of Δt_i^* should be chosen as large as possible without risking significant effects related to the walls. For calculating the values of D_{obs} presented here, the selection of Δt_i^* in each experimental run was governed by several considerations: (i) Δt_i^* was taken sufficiently large for the curve of D_{obs} *vs.* Δt_i^* to have become relatively flat, thus indicating that the passing and sighting errors were within reasonable bounds; (ii) Δt_i^* was not allowed to become so large that the distribution of Δy_i failed a chi-square test for normal distribution, since such failure would indicate proximity to a wall; and (iii) Δt_i^* was kept small enough so that the corresponding diffusion length (for the observed value of D) was no greater than a modest fraction of the channel half-width.

5. Results

From the foregoing considerations of errors it became clear that D could not be established with a high degree of accuracy. Since the several sources of error could be assessed only roughly, and since they were at least partially self-cancelling, it did not seem advantageous to attempt corrections of the raw data.

Thus the results finally presented in figure 2 are based on the average values of ω and ϕ as discussed previously, and were calculated with appropriate values of Δt_i^* as described previously. We believe that the results shown in figure 2 are accurate to within a factor of two. While one might regret not having a higher level of accuracy, these results are believed to be significant for two reasons: first, they establish with reasonable certainty the order of magnitude of the self-diffusion coefficient for particles of equal size; and second no theory, not even a crude one, currently exists for this type of self-diffusion.

The large scatter of data in figure 2 is due, we think, to the nature and size of the experimental errors rather than to the parameters in (2) neglected. There is no ordering with respect to particle Reynolds number. At a concentration of 0·40, for instance, the uppermost and lowermost points have the two lowest Reynolds numbers.

Noting that $D/a^2\omega$ must be zero when $\phi = 0$, figure 2 shows that $D/a^2\omega$ seems to increase approximately linearly with ϕ up to about $\phi \cong 0{\cdot}2$. Beyond this, the

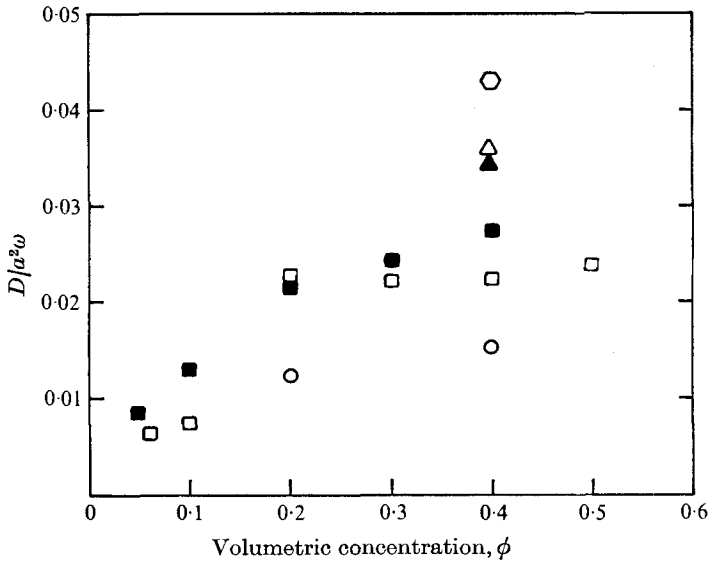

FIGURE 2. Experimental results.

	■	▲	□	△	⬡	○
Particle	Disk	Disk	Sphere	Sphere	Sphere	Sphere
a (cm)	0·16	0·16	0·16	0·16	0·16	0·05
ω (s^{-1})	10	1	10	1	0·4	10
$a^2\omega$ ($cm^2\ s^{-1}$)	0·256	0·0256	0·256	0·0256	0·0102	0·025

scatter and inaccuracies preclude any conclusion as to the effect of ϕ. Perhaps the most one can now say for $\phi > 0{\cdot}2$ is that $D/a^2\omega$ is of the order of 0·025.

Finally, there seems to be no significant separation of the results for the spheres and the disks. For equal values of the major diameter, the self-diffusion coefficient appears to be similar in magnitude for these two quite different shapes, a result perhaps not unexpected from what we know of inertia-free flows. This is significant with regard to red blood cells, which are extremely complex in shape, but somewhat disk-like. One might also venture the guess that the variation in shape of the red blood cell by reason of its deformability has little effect on D, but this is more uncertain.

Financial support for this research was received from the National Science Foundation (Grant GK-31183, Engineering Mechanics Program) and from the National Heart and Lung Institute (PHS Grant 5P01H14322-03 to the Harvard–MIT Program in Health Science and Technology). Dr William Hyman made an important contribution to the early phases of the investigation. Acknowledgement is made to D. Moluchnik of the Shipley Co. for copper-coating the spheres, to the MIT Radiation Protection Office for aid in working with ^{58}Co, and to D. Palmer and R. Fenner of the Fluid Mechanics Laboratory for construction of apparatus. Prof. C. C. Colton and Prof. B. B. Mikic provided helpful comments as the investigation proceeded.

REFERENCES

BAILEY, D. G. 1975 Migrations of disks in Couette flow and application to blood oxygenator design. Mech. Eng. thesis, Massachusetts Institute of Technology.

BATCHELOR, G. K. 1974 Transport properties of two-phase materials with random structure. *Ann. Rev. Fluid Mech.* **6**, 227.

BERNSTEIN, E. F., BLACKSHEAR, P. L. & KELLER, K. H. 1967 Factors influencing erythrocyte destruction in artificial organs. *Am. J. Surgery*, **114**, 126.

BRENNER, H. 1970 Rheology of two-phase systems. *Ann. Rev. Fluid Mech.* **2**, 137.

BRENNER, H. 1963 The Stokes resistance of an arbitrary particle. *Chem. Engng Sci.* **18**, 2.

BRETHERTON, F. P. 1962 The motion of rigid particles in a shear flow at low Reynolds number. *J. Fluid Mech.* **14**, 284.

BUYEVICH, YU. A. 1972 Statistical hydromechanics of disperse systems. Part 3. Pseudo-turbulent structure of homogeneous suspensions. *J. Fluid Mech.* **56**, 313.

CHANDRASEKHAR, S. 1943 Stochastic problems in physics and astronomy, *Rev. Mod. Phys.* **15**, 1. (See also *Selected Papers on Noise and Stochastic Processes* (ed. Nelson Wax), p. 3. Dover, 1954.)

CHARM, S. E. 1974 *Blood Flow and Microcirculation*. Wiley.

COLLINGHAM, R. E. 1968 Mass transfer in flowing suspensions. Ph.D. thesis, University of Minnesota.

COLTON, C. K. 1976 Fundamentals of gas transport in blood. In *Membrane, Artificial Lungs, and Acute Respiratory Failure* (ed. W. M. Zapol & J. Qvisp), p. 3. Hemisphere Publ. Co., Washington D.C.

COPLEY, A. L. 1966 *Hemorheology*.

COX, R. G. & MASON, S. G. 1971 Suspended particles in fluid flow through tubes. *Ann. Rev. Fluid Mech.* **3**, 291.

DILLER, T. E. 1974 Augmentation of oxygen diffusion in blood due to shear induced red blood cell motion. S.M. thesis, Massachusetts Institute of Technology.

ECKSTEIN, E. C. 1975 Particle migration in a linear shear flow. Ph.D. thesis, Massachusetts Institute of Technology.

FUNG, Y. C. 1969 Blood flow in the capillary bed. *J. Biomech.* **2**, 353.

GOLDSMITH, H. L. & MASON, S. G. 1967 The microrheology of dispersions. In *Rheology – Theory and Applications*, vol. 4 (ed. F. R. Eirich). Academic.

GRABOWSKI, E. F., FRIEDMAN, L. I & LEONARD, E. F. 1972 Effects of shear rate on the diffusion and adhesion of blood platelets to a foreign surface. *Ind. Engng Chem. Fundam.* **11**, 224.

HAPPEL, J. & BRENNER, H. 1973 *Low Reynolds Number Hydrodynamics*. Noordhoff.

HILL, J. D., IATRIDIS, A., O'KEEFE, R. & KITRILAKIS, S. 1974 Technique for achieving high gas exchange rates in membrane oxygenation. *Trans. A.S.A.I.O.* **20**, 249.

HO, B. P. & LEAL, L. G. 1974 Inertial migration of rigid spheres in two-dimensional unidirectional flows. *J. Fluid Mech.* **65**, 365.

JEFFERY, G. B. 1922 The motion of ellipsoidal particles immersed in a viscous fluid. *Proc. Roy. Soc.* A **102**, 161.

KARNIS, A., GOLDSMITH, H. L. & MASON, S. G. 1966*a* The kinetic of flowing dispersions; I. Concentrated suspensions of rigid particles. *J. Colloid Interface Sci.* **22**, 531.

KARNIS, A., GOLDSMITH, H. L. & MASON, S. G. 1966*b* The flow of suspensions through tubes; V. Inertial effects. *Can. J. Chem. Engng* **44**, 181.

KELLER, K. H. 1971 Effect of fluid shear on mass transport in flowing blood, *Fed. Proc.* **30**, 1591.

MERRILL, E. W., GILLILAND, E. R., COKELET, G., SHEN, H., BRITTEN, A. & WELLS, R. E. 1963 Rheology of human blood near and at zero flow. Effects of temperature and hematocrit level. *Biophys. J.* **3**, 199.

PETSCHEK, H. E. & WEISS, R. F. 1970 Hydrodynamic problems in blood coagulation. *A.I.A.A. Paper*, no. 70–143.

SACKS, A. H. & TICKNER, E. G. 1967 Laminar flow regimes for rigid-sphere suspensions. In *Hemorheology, Proc. 1st Int. Conf.*, p. 277. Pergamon.

SEGRÉ, G. & SILBERBERG, A. 1962 Behaviour of macroscopic rigid spheres in Poiseuille flow. *J. Fluid Mech.* **14**, 115, 136.

STEINBACH, J. H. 1974 Red cell diffusion measurements by the Taylor dispersion method. Ph.D. thesis, University of Minnesota.

TAYLOR, G. I. 1953 Dispersion of soluble matter in solvent flowing slowly through a tube. *Proc. Roy. Soc.* A **219**, 186.

TURITTO, V. T., BENIS, A. M. & LEONARD, E. F. 1972 Platelet diffusion in flowing blood. *Ind. Engng Chem. Fund.* **11**, 216.

VAND, V. 1948 Viscosity of solutions and suspensions. I. Theory. *J. Phys. Colloid. Chem.* **52**, 277.

WHITMORE, R. L. 1963 Hemorheology and hemodynamics. *Biorheol.* **1**, 20.

WOHL, P. R. & RUBINOW, S. I. 1974 The transverse force on a drop in an unbounded parabolic flow. *J. Fluid Mech.* **62**, 185.